



RESEARCH ARTICLE

Relationship between regional gray matter volumes and dopamine D₂ receptor and transporter in living human brains

Shin Kurose^{1,2}  | Manabu Kubota^{1,3}  | Keisuke Takahata^{1,2} |
 Yasuharu Yamamoto^{1,2}  | Hironobu Fujiwara³ | Yasuyuki Kimura⁴ | Hiroshi Ito⁵ |
 Hiroyoshi Takeuchi² | Masaru Mimura² | Tetsuya Suhara¹ | Makoto Higuchi¹

¹Department of Functional Brain Imaging, National Institute of Radiological Sciences, National Institutes for Quantum and Radiological Science and Technology, Chiba, Japan

²Department of Neuropsychiatry, Keio University School of Medicine, Tokyo, Japan

³Department of Psychiatry, Kyoto University Graduate School of Medicine, Kyoto, Japan

⁴Department of Clinical and Experimental Neuroimaging, Center for Development of Advanced Medicine for Dementia, National Center for Geriatrics and Gerontology, Obu, Japan

⁵Department of Radiology and Nuclear Medicine, Fukushima Medical University, Fukushima, Japan

Correspondence

Manabu Kubota, Department of Functional Brain Imaging, National Institute of Radiological Sciences, National Institutes for Quantum and Radiological Science and Technology, 4-9-1 Anagawa, Inage-ku, Chiba, 263-8555, Japan.

Email: kubota.manabu@qst.go.jp; m_kubota@kuhp.kyoto-u.ac.jp

Funding information

Japan Agency for Medical Research and Development, Grant/Award Numbers: 19dm0307105, 20dm0207072; Japan Society for the Promotion of Science, Grant/Award Number: 19K17101

Abstract

Although striatal dopamine neurotransmission is believed to be functionally linked to the formation of the corticostriatal network, there has been little evidence for this regulatory process in the human brain and its disruptions in neuropsychiatric disorders. Here, we aimed to investigate associations of striatal dopamine transporter (DAT) and D₂ receptor availabilities with gray matter (GM) volumes in healthy humans. Positron emission tomography images of D₂ receptor ($n = 34$) and DAT ($n = 17$) captured with the specific radioligands [¹¹C]raclopride and [¹⁸F]FE-PE2I, respectively, were acquired along with T1-weighted magnetic resonance imaging data in our previous studies, and were re-analyzed in this work. We quantified the binding potentials (BP_{ND}) of these radioligands in the limbic, executive, and sensorimotor functional subregions of the striatum. Correlations between the radioligand BP_{ND} and regional GM volume were then examined by voxel-based morphometry. In line with the functional and anatomical connectivity, [¹¹C]raclopride BP_{ND} in the limbic striatum was positively correlated with volumes of the uncus/parahippocampal gyrus and adjacent temporal areas. Similarly, we found positive correlations between the BP_{ND} of this radioligand in the executive striatum and volumes of the prefrontal cortices and their adjacent areas as well as between the BP_{ND} in the sensorimotor striatum and volumes of the somatosensory and supplementary motor areas. By contrast, no significant correlation was found between [¹⁸F]FE-PE2I BP_{ND} and regional GM volumes. Our results suggest unique structural and functional corticostriatal associations involving D₂ receptor in healthy humans, which might be partially independent of the nigrostriatal pathway reflected by striatal DAT.

KEYWORDS

D₂ receptor, dopamine transporter, gray matter, MRI, PET, striatum

This is an open access article under the terms of the Creative Commons Attribution-NonCommercial-NoDerivs License, which permits use and distribution in any medium, provided the original work is properly cited, the use is non-commercial and no modifications or adaptations are made.

© 2021 The Authors. *Human Brain Mapping* published by Wiley Periodicals LLC.

1 | INTRODUCTION

There is growing evidence for reciprocal and functional relationships between dopamine neurotransmission and the corticostriatal network. Striatal dopamine release modulates corticostriatal plasticity (Reynolds & Wickens, 2002), while repetitive transcranial magnetic stimulation (rTMS) of the prefrontal (Strafella, Paus, Barrett, & Dagher, 2001) and motor cortices (Strafella, Paus, Fraraccio, & Dagher, 2003) can induce dopamine release in the human striatum.

In several neuropsychiatric diseases, including schizophrenia (Abi-Dargham et al., 2000; Caravaggio, Borlido, Wilson, & Graff-Guerrero, 2015; Kegeles et al., 2010; Yao et al., 2013), impairments in both dopamine neurotransmission and the corticostriatal network are manifested, along with alterations in brain morphology (Honea, Crow, Passingham, & Mackay, 2005; Shepherd, Laurens, Matheson, Carr, & Green, 2012). Until now, however, only a few positron emission tomography (PET) studies have investigated the associations between brain morphology and dopaminergic statuses in humans (Caravaggio et al., 2017; Woodward et al., 2009), and their relationships in the healthy versus diseased brains remain largely unresolved. In addition, because dopamine neurons constitute cortico-subcortical networks, rather than focusing on specific cortical or subcortical regions, it might be more beneficial to focus on a wide range of such regions to clarify the relationship between brain morphology and dopaminergic statuses in the striatum. However, these previous imaging studies were limited to intercortical or intersubcortical analysis. Further, functional and morphometric assays of the striatum are generally performed based on its anatomical subdivisions, including the caudate, putamen, and nucleus accumbens, but these structures are comprised of cytoarchitecturally undifferentiated areas (Tziortzi et al., 2014). Nonhuman nerve fiber tracing and human imaging studies have shown that the striatum could be divided into three functional subdivisions—the executive, sensorimotor, and limbic striatum—with distinct distributions of their cortical inputs onto single striatal neurons, forming monosynaptic contacts (Draganski et al., 2008; Haber, 2003; Parent & Hazrati, 1995; Wall, De La Parra, Callaway, & Kreitzer, 2013). Use of the connectivity-based functional striatal subregions would be beneficial for a better understanding of such a relationship, which could reflect the corticostriatal network, although it should be noted that several functionally related cortical areas send partially overlapping projections to certain striatal areas (Alexander, DeLong, & Strick, 1986). Indeed, a previous study with diffusion-weighted magnetic resonance imaging (MRI) and PET has suggested that regional differences in the striatal dopamine status could be evaluated in greater detail on the basis of connectivity-based functional subdivision of the striatum (Tziortzi et al., 2014).

Among the components of dopamine neurotransmission, several animal studies have shown that stimulation of dopamine D₂ receptors promotes the outgrowth of neurites in cerebral cortical neurons (Hasbi et al., 2009; Todd, 1992). In contrast, knockout mice of dopamine transporters (DAT) showed little morphological changes (Zhang et al., 2010). As for the relationship between dopamine D₂ receptors and DATs, animal studies showed reciprocal actions between them,

while there had been no comprehensive studies to examine the relationship in humans (Bolan et al., 2007; Chen et al., 2006; Courtney & Ford, 2014; Lee et al., 2007). Based on these findings, we hypothesized that brain morphology might be more related to availabilities of D₂ receptors than DATs, and that there might be some relationship between availabilities of D₂ receptors and DATs.

The aim of this study was (1) to examine the relationship between regional gray matter (GM) volumes and availabilities of dopamine D₂ receptors and DATs in the striatal subregions divided based on the functional connectivity in healthy humans (Tziortzi et al., 2014) and (2) to investigate the relationship between availabilities of dopamine D₂ receptors and those of DATs in the striatum.

2 | MATERIALS AND METHODS

2.1 | Subjects

We collected data from neuroimaging datasets in our two previous clinical studies ([UMIN000008232] (Kimura et al., 2017), [UMIN000007240]), which had been registered in the University Hospital Medical Information Network Clinical Trials Registry. The participants were 34 nonsmoking male volunteers (age, 23 ± 1.9 years; body mass index, 20.9 ± 1.9 kg/m²; mean \pm SD). By a board-certified psychiatrist, we confirmed that all subjects were free of both current and past medical and neuropsychiatric illnesses based on their medical histories and physical examinations, and also of current use of psychoactive drug/medication.

This study was approved by the Institutional Review Board of the National Institutes for Quantum and Radiological Science and Technology, Chiba, Japan, and was performed in accordance with the ethical standards established in the 1964 Declaration of Helsinki and its later amendments. Written informed consent was obtained from all subjects before their inclusion in the study.

2.2 | PET procedures

All subjects underwent a PET scan with [¹¹C]raclopride, a D_{2/3} receptor radioligand. Among them, 17 individuals (age, 22 ± 0.9 years) also completed a PET scan with [¹⁸F]FE-PE2I, a DAT radioligand. Injection doses of [¹¹C]raclopride and [¹⁸F]FE-PE2I were 222.1 ± 15.5 MBq and 185.3 ± 20.7 MBq, respectively, and molar activities of [¹¹C]raclopride and [¹⁸F]FE-PE2I were 210.0 ± 61.7 GBq/ μ mol and 410.5 ± 319.1 GBq/ μ mol, respectively. With regard to the 17 subjects undergoing both the PET scans with [¹¹C]raclopride and [¹⁸F]FE-PE2I, [¹⁸F]FE-PE2I PET scan was begun 2 hr after the start of [¹¹C]raclopride PET. PET images were acquired using a PET camera (SET-3000GCT/X, Shimadzu, Kyoto, Japan), with the imaging session consisting of 35 frames of increasing duration from 30 s to 5 min over 60 min for [¹¹C]raclopride and 38 frames over 90 min for [¹⁸F]FE-PE2I. Scatter correction was performed by a hybrid scatter correction method based on acquisition with dual-energy window setting

(Ishikawa et al., 2005). A 4-min transmission scan using a ^{137}Cs line source was obtained to correct for attenuation.

2.3 | MRI procedures and preprocessing

All MRI scans were performed with a 3-T MRI scanner (MAGNETOM Verio, Siemens, Germany). 3D volumetric acquisition of a T1-weighted gradient echo sequence produced a gapless series of thin sagittal sections. The scan parameters for our participants were either of the following sets: (1) TE, 9.2 ms; TR, 21 ms; flip angle, 30° ; and slice thickness, 1 mm ($n = 17$; subjects who completed both [^{11}C]raclopride and [^{18}F]FE-PE2I PET; UMIN000008232; Kimura et al., 2017); or (2) TE, 3.43 ms; TR, 2300 ms; flip angle, 30° ; and slice thickness, 1 mm ($n = 17$; subjects who completed [^{11}C]raclopride PET only) (UMIN000007240).

MRI data were processed and analyzed using statistical parametric mapping (SPM12, Wellcome Trust Centre for Neuroimaging, London, UK) software, specifically using Diffeomorphic Anatomical Registration Through Exponentiated Lie algebra (DARTEL) toolbox running on Matlab R2018b (MathWorks, MA; Ashburner, 2007). In the segmentation procedure, brain structures were classified into GM, white matter (WM), and cerebrospinal fluid (CSF), which were resliced into $1.5 \times 1.5 \times 1.5$ mm voxels. We created a customized template from the images of all participants. The GM images were spatially normalized into the standardized Montreal Neurological Institute (MNI) 152 brain template. The voxel values of segmented and normalized GM images were modulated by the Jacobian determinants obtained from a nonlinear normalization step. In the smoothing procedure, a Gaussian kernels filter was used to smoothen normalized images. The kernel size of the Gaussian filter was set to 8 mm in full-width at half-maximum (FWHM).

2.4 | Quantification of PET images

PET data processing was conducted using PMOD 3.8 (PMOD Technologies Ltd., Zurich, Switzerland).

All PET images were reconstructed using the filtered back-projection method (Gaussian filter, kernel 5 mm; reconstructed in-plane resolution 7.5 mm at FWHM; voxel size $2 \times 2 \times 2.6$ mm). Motion-corrected PET images were co-registered to corresponding individual MR images. All PET images were spatially normalized to MNI152 standard space, based on parameters for the transformation of individual MR images into the template estimated by DARTEL SPM12. The striatal and cerebellar ROIs along with normalized MRI and PET images of a single subject are illustrated in Figure S1.

Quantitative analysis was then performed by applying a simplified reference tissue model (SRTM; Alakurtti et al., 2015; Boileau et al., 2013; Lammertsma & Hume, 1996; N. B. Urban et al., 2012) to the time course of radioactivity concentrations in the striatal subregions using the cerebellar cortex as reference tissue. Availabilities of D_2 receptors and DATs were quantified as binding potentials relative to the nondisplaceable

tissue (BP_{ND}) of [^{11}C]raclopride and [^{18}F]FE-PE2I, respectively. A connectivity-based probabilistic atlas of the striatum (Tziortzi et al., 2014) was applied to the spatially normalized PET images to determine BP_{ND} values in the limbic, executive, and sensorimotor striatal subregions. We used the atlas of the cerebellar lobules in MNI152 standard space (Diedrichsen, Balsters, Flavell, Cussans, & Ramnani, 2009).

Additionally, we performed partial volume correction (PVC) using the Müller-Gärtner approach (Müller-Gärtner et al., 1992), as in previous studies (Ito et al., 2014; Mecca et al., 2018; Mecca et al., 2020). For each dynamic PET frame, GM voxels were corrected for spill-in and spill-out of activity, assuming that activity in CSF was 0 and WM activity was uniform and was estimated from each image time frame.

2.5 | Data analysis

2.5.1 | Correlations between local GM volume and BP_{ND} of [^{11}C]raclopride and [^{18}F]FE-PE2I

We investigated correlations between the local GM volume and BP_{ND} of [^{11}C]raclopride and [^{18}F]FE-PE2I in the three striatal subregions while controlling for age, total brain volume, and MRI parameters, using voxel-based morphometry (VBM) implemented in SPM12 running on Matlab R2018b (J. Ashburner & Friston, 2000). The statistical significance threshold for VBM was set at $p < .001/3$ at peak levels, which was corrected for the three striatal subregions. We performed VBM analysis because VBM allows the investigation of GM regions of the whole brain without bias, and thus might be more suitable for exploratory studies.

We conducted the following additional analyses to examine whether the associations between availabilities of D_2 receptors and brain morphology were explained by DAT or not. First, the regional GM volume data (eigenvariates) were extracted from the above-mentioned clusters significantly correlated with the BP_{ND} values of [^{11}C]raclopride in the 34 subjects. Namely, from our VBM results, we extracted (1) eigenvariates from clusters significantly correlated with the limbic striatal BP_{ND} of [^{11}C]raclopride, (2) eigenvariates from clusters significantly correlated with the executive striatal BP_{ND} of [^{11}C]raclopride, and (3) eigenvariates from clusters significantly correlated with the sensorimotor striatal BP_{ND} of [^{11}C]raclopride, respectively. We performed a correlational analysis between the BP_{ND} values of [^{11}C]raclopride and the regional GM volume data (eigenvariates) for each striatal subregion, respectively, in (1) all subjects ($n = 34$), and (2) subjects undergoing both [^{11}C]raclopride and [^{18}F]FE-PE2I PET scans ($n = 17$), respectively. Next, in these 17 subjects, we performed a partial correlational analysis for the above correlations while controlling for the BP_{ND} values of [^{18}F]FE-PE2I. Further, we performed a correlational analysis between the BP_{ND} values of [^{18}F]FE-PE2I and the regional GM volume data (eigenvariates) for each striatal subregion in subjects undergoing both [^{11}C]raclopride and [^{18}F]FE-PE2I PET scans ($n = 17$). The statistical significance threshold was set at $p < .05/3$ in these analyses. Data were analyzed by using the Statistical Package for Social Sciences (SPSS) version 25 (SPSS, Inc., Chicago, IL).

2.5.2 | Correlations between the BP_{ND} of [^{11}C]raclopride and [^{18}F]FE-PE2I

We examined correlations between the BP_{ND} of [^{11}C]raclopride and [^{18}F]FE-PE2I in each striatal subregion by correlational analysis, with a statistical significance threshold of $p < .05/3$. Data were analyzed by using SPSS.

3 | RESULTS

3.1 | Correlations between local GM volume and BP_{ND} of [^{11}C]raclopride

We found significant positive correlations of [^{11}C]raclopride BP_{ND} in the limbic striatum with GM volumes in a limbic area, including the uncus/parahippocampal cortex [Brodmann's area (BA) 36], and adjacent temporal cortices (BA 20, 21, 38), along with the declive of the cerebellum (Table 1 and Figure 1). Likewise, a significant positive correlation was observed between [^{11}C]raclopride BP_{ND} in the executive striatum and GM volumes in regions associated with executive functions, such as prefrontal (BA 8, 9, 10) cortices, and an area adjacent to the prefrontal cortex (BA 6, 32), along with a parietal cortical region

(BA 40) (Table 1 and Figure 1b). Moreover, [^{11}C]raclopride BP_{ND} in the sensorimotor striatum was significantly and positively correlated with GM volumes in regions associated with sensorimotor functions, such as the supplemental motor (BA 6) and somatosensory (BA 40) cortices and an area adjacent to the premotor cortex (BA 8, 9), as well as the frontal pole (BA 10) and lingual (BA 18) gyri (Table 1 and Figure 1c).

Results after applying PVC were as follows: there were positive correlations between (1) [^{11}C]raclopride BP_{ND} in the limbic striatum and GM volumes in temporal cortices adjacent to the limbic area (BA 20, 38), (2) [^{11}C]raclopride BP_{ND} in the executive striatum and GM volumes in medial frontal (BA 9) and postcentral (BA 3) cortices, along with inferior temporal (BA 19) cortices, and (3) [^{11}C]raclopride BP_{ND} in the sensorimotor striatum and GM volumes in regions associated with sensorimotor functions, such as postcentral (BA 3) cortices, as well as the cingulate (BA 24) and medial frontal (BA 10) cortices.

In all subjects, significant positive correlations were found between the BP_{ND} values of [^{11}C]raclopride and eigenvariables for the limbic ($p = .011$, Pearson's $r = .43$), executive ($p = .001$, $r = .53$), and sensorimotor ($p = .001$, $r = .54$) subregions of the striatum, respectively (Figure 2).

In the 17 subjects undergoing PET scans with both [^{11}C]raclopride and [^{18}F]FE-PE2I, significant positive correlations were

TABLE 1 Local maxima of positive correlations between [^{11}C]raclopride BP_{ND} in the subregion of the striatum and regional GM volumes

Subregion of the striatum	Brain region	Talairach coordinates			p -value at the peak level		p -value at the cluster level	
		X	Y	Z	Uncorrected	FWE	Uncorrected	
Limbic	Right middle temporal gyrus (BA 21)	42	6	-36	<.00033	.034	.014	421
	Left inferior temporal gyrus (BA 20)	-48	-4	-27	<.00033	.352	.149	126
	Left cerebellum, posterior lobe, declive	-28	-78	-22	<.00033	.396	.026	336
	Right limbic lobe, uncus (BA 36)	26	-10	-33	<.00033	.516	.161	118
	Left superior temporal gyrus (BA 38)	-30	6	-39	<.00033	.64	.005	581
Executive	Left medial frontal gyrus (BA 9)	-16	32	27	<.00033	.029	.018	383
	Right medial frontal gyrus (BA 6)	14	-4	54	<.00033	.214	.307	61
	Right medial frontal gyrus (BA 10)	20	46	3	<.00033	.238	.249	78
	Right inferior parietal lobule (BA 40)	40	-30	48	<.00033	.608	.025	339
	Right inferior parietal lobule (BA 40)	51	-57	51	<.00033	.688	.243	80
	Left anterior cingulate (BA 32)	-20	44	8	<.00033	.764	.292	65
	Left postcentral gyrus (BA 2)	-40	-20	32	<.00033	.831	.285	67
	Left medial frontal gyrus (BA 8)	-9	33	45	<.00033	.881	.337	54
Sensorimotor	Right medial frontal gyrus (BA 6)	12	-18	57	<.00033	.195	.069	208
	Right medial frontal gyrus (BA 10)	18	46	4	<.00033	.241	.337	54
	Left lingual gyrus (BA 18)	-14	-74	-6	<.00033	.413	.167	114
	Left medial frontal gyrus (BA 9)	-18	30	27	<.00033	.502	.114	152
	Right medial frontal gyrus (BA 8)	12	38	40	<.00033	.598	.274	70
	Right postcentral gyrus (BA 40)	42	-30	50	<.00033	.656	.007	520

Note: Statistical significance threshold for VBM was set as $p < .001/3$ (uncorrected) at the peak level represented in bold. Voxel size $1.5 \times 1.5 \times 1.5$ mm². Extent threshold: 50 voxels.

Abbreviations: BA, Brodmann's area; FWE, family-wise error.

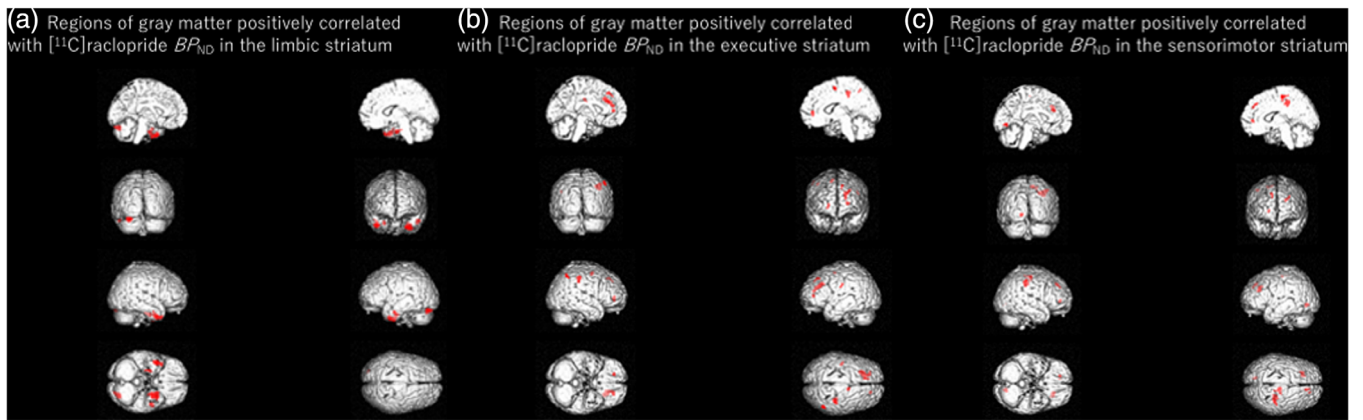


FIGURE 1 (a) Regions of gray matter positively correlated with [^{11}C]raclopride BP_{ND} in the limbic striatum. (b) Regions of gray matter positively correlated with [^{11}C]raclopride BP_{ND} in the executive striatum. (c) Regions of gray matter positively correlated with [^{11}C]raclopride BP_{ND} in the sensorimotor striatum. The statistical significance threshold was set at $p < .001/3$ (uncorrected) at the peak levels, with a 50-voxel extent threshold

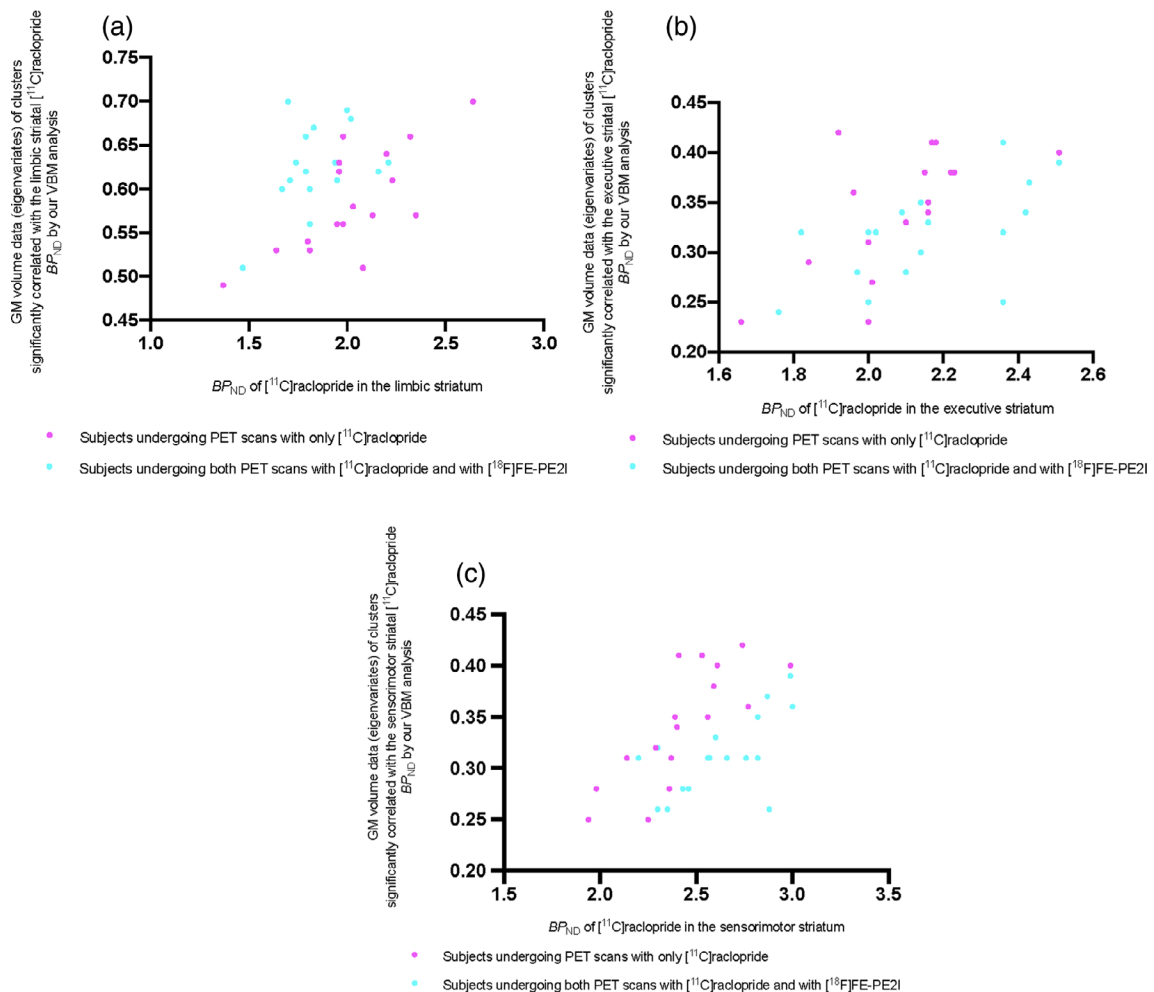


FIGURE 2 (a) Scatter plot of [^{11}C]raclopride BP_{ND} in the limbic striatum against regional gray matter (GM) volume data (eigenvariates; $n = 34$). The GM volume data (eigenvariates) were extracted from the clusters significantly correlated with the limbic striatal BP_{ND} of [^{11}C]raclopride in our VBM results shown in Figure 1a. (b) Scatter plot of [^{11}C]raclopride BP_{ND} in the executive striatum against regional GM volume data (eigenvariates; $n = 34$). The GM volume data (eigenvariates) were extracted from the clusters significantly correlated with the executive striatal BP_{ND} of [^{11}C]raclopride in our VBM results shown in Figure 1b. (c) Scatter plot of [^{11}C]raclopride BP_{ND} in the sensorimotor striatum against regional GM volume data (eigenvariates; $n = 34$). The GM volume data (eigenvariates) were extracted from the clusters significantly correlated with the sensorimotor striatal BP_{ND} of [^{11}C]raclopride in our VBM results shown in Figure 1c

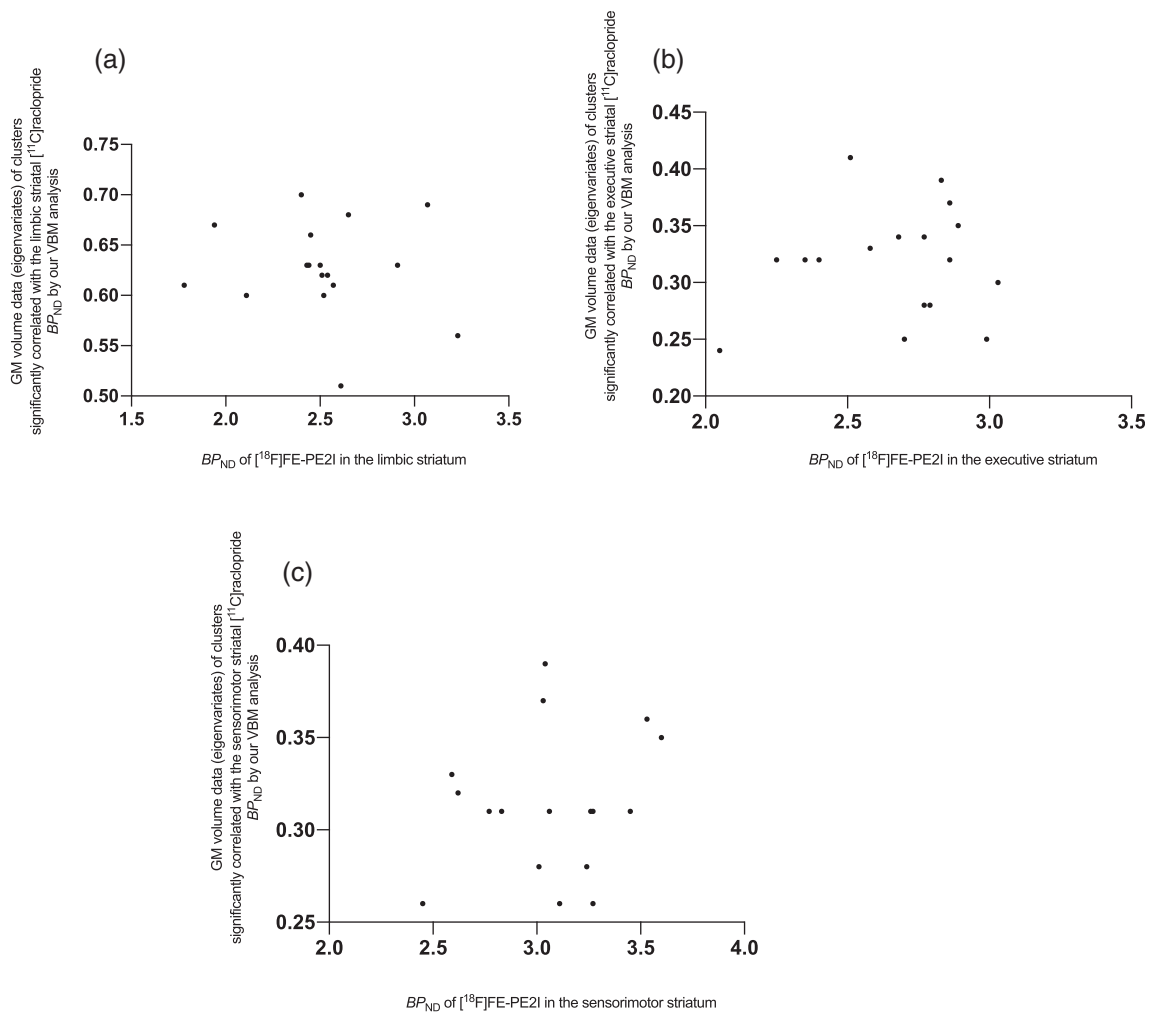


FIGURE 3 (a) Scatter plot of $[^{18}\text{F}]$ FE-PE2I BP_{ND} in the limbic striatum against regional gray matter (GM) volume data (eigenvariates; $n = 34$). The GM volume data (eigenvariates) were extracted from the clusters significantly correlated with the limbic striatal BP_{ND} of $[^{11}\text{C}]$ raclopride in our VBM results shown in Figure 1. (b) Scatter plot of $[^{18}\text{F}]$ FE-PE2I BP_{ND} in the executive striatum against regional GM volume data (eigenvariates; $n = 34$). The GM volume data (eigenvariates) were extracted from the clusters significantly correlated with the executive striatal BP_{ND} of $[^{11}\text{C}]$ raclopride in our VBM results shown in Figure 1b. (c) Scatter plot of $[^{18}\text{F}]$ FE-PE2I BP_{ND} in the sensorimotor striatum against regional GM volume data (eigenvariates; $n = 34$). The GM volume data (eigenvariates) were extracted from the clusters significantly correlated with the sensorimotor striatal BP_{ND} of $[^{11}\text{C}]$ raclopride in our VBM results shown in Figure 1c

found between the BP_{ND} values of $[^{11}\text{C}]$ raclopride and the eigenvariates for the executive ($p = .003$, $r = .67$) and sensorimotor ($p = .007$, $r = .62$) subregions of the striatum, respectively, while a correlation between these parameters for the limbic striatum showed a trend toward significance ($p = .116$, $r = .40$) (Figure 2).

Partial correlational analyses also revealed significant positive correlations between the BP_{ND} values of $[^{11}\text{C}]$ raclopride and the eigenvariates for the executive ($p = .001$, $r = .75$) and sensorimotor ($p = .006$, $r = .66$) subregions of the striatum, respectively, while a correlation between these parameters for the limbic striatum showed a trend toward significance ($p = .067$, $r = .47$).

On the other hand, there were no significant correlations between the BP_{ND} values of $[^{18}\text{F}]$ FE-PE2I and the eigenvariates for any of the striatal subregions (Figure 3).

3.2 | Correlations between local GM volume and BP_{ND} of $[^{18}\text{F}]$ FE-PE2I

By contrast to the above VBM results using $[^{11}\text{C}]$ raclopride BP_{ND} , no significant correlation was found between regional GM volume and BP_{ND} of $[^{18}\text{F}]$ FE-PE2I.

3.3 | Correlations between the BP_{ND} of $[^{11}\text{C}]$ raclopride and $[^{18}\text{F}]$ FE-PE2I

There were significant positive correlations between the BP_{ND} values of $[^{11}\text{C}]$ raclopride and of $[^{18}\text{F}]$ FE-PE2I in the executive ($p = .005$, $r = .65$) and sensorimotor ($p = .014$, $r = .58$) subregions of the

striatum, while no significant correlation was found between these parameters in the limbic striatum ($p = .18$, $r = .34$).

4 | DISCUSSION

We have demonstrated positive correlations between dopamine $D_{2/3}$ receptor radioligand BP_{ND} in the functional subregions of the striatum and the GM volumes of regions that could be functionally and anatomically connected to each of these striatal subdomains. Meanwhile, no marked correlations were observed between DAT radioligand BP_{ND} and regional GM volumes. Before and after applying the PVC, generally there were no noticeable differences in the results (although slight differences were found for the executive striatum).

To date, only a few studies have investigated the relationship between brain morphology and the dopamine system in healthy humans. A previous PET study has reported associations between cortical thickness and dopamine release in striatal subregions; greater amphetamine-induced changes in [^{11}C]raclopride BP_{ND} were observed in the ventral limbic striatum, and they were associated with thinner frontal cortices (Jaworska et al., 2017). With regard to the relationship between brain morphology and D_2 receptor availability, there were only two studies, and the findings were inconsistent (Caravaggio et al., 2017; Woodward et al., 2009). Namely, one of these two PET studies with [^{18}F]fallypride has demonstrated a positive intraregional correlation between $D_{2/3}$ receptor availability and the GM volume within the caudate, thalamus, and amygdala in healthy human brains (Woodward et al., 2009). The other exploratory clinical PET study with two $D_{2/3}$ receptor radioligands, [^{11}C]raclopride and [^{11}C]-(+)-PHNO, in healthy individuals reported that BP_{ND} of [^{11}C]-(+)-PHNO but not [^{11}C]raclopride was positively correlated with the local volume within anatomical striatal subregions except for the putamen (Caravaggio et al., 2017). Unlike those within-region analyses, the present work explored the relationship between the morphology across GM regions and the striatal dopamine system in healthy humans. Furthermore, we focused on the connections from cortical inputs and functionally distinct striatal subdivisions, leading to revelation of the associations between the morphology and dopaminergic components via the corticostriatal circuits. We did not find any significant associations between GM volumes within the striatum and D_2 receptor availabilities, unlike those previous studies (Caravaggio et al., 2017; Woodward et al., 2009). Possible interpretations might be due to the difference in radioligands, that is, [^{11}C]raclopride in Caravaggio et al. and our study vs. [^{11}C]-(+)-PHNO in Caravaggio et al. and [^{18}F]fallypride in Woodward et al: differences in selectivity for D_2 versus D_3 receptors or in affinity for endogenous dopamine among these radioligands (Gallezot et al., 2012; Mukherjee et al., 2002). Otherwise, it might be due to differences in demographic data (e.g., male ratio: 100% in our study, 53% in Woodward et al., 63% in Caravaggio et al.; age: 23 ± 1.9 years in our study, 24 ± 5.5 in Woodward et al., 39 ± 14.5 for [^{11}C]raclopride and 39 ± 14.6 for [^{18}F]fallypride in Caravaggio et al.). In the current study, we targeted the GM volume among several morphometric measures. As the present study was for

exploratory research, we did not investigate the relationship between these dopamine neurotransmissions and functional/structural connectivity. Future studies will be needed to examine the relationship between dopamine neurotransmission, cortical thickness/surface area/volume, and functional/structural connectivity in greater detail.

In consideration of the availabilities of D_2 and D_3 receptors and affinities of [^{11}C]raclopride for these target molecules, it is conceivable that PET data with this radioligand is primarily indicative of the D_2 receptor availability in the striatum. Hence, the positive correlation between [^{11}C]raclopride BP_{ND} in the limbic, executive, and sensorimotor striatal subregions and GM volumes of functionally connected cortices could imply the roles of dopamine as a morphogen in the formation and preservation of the cortical networks mediated by striatal D_2 receptors. Indeed, a previous in-vitro study demonstrated that a D_2 receptor agonist stimulated the outgrowth of neurites in cerebral cortical neurons, whereas a D_2 receptor antagonist abolished it (Todd, 1992). Therefore, D_2 receptors on presynaptic terminals of the cortical inputs in the striatum are likely to retrogradely elicit the generation and extension of neuritic processes, resulting in an enlarged cortical morphology. A combined in-vitro neuronal culture and in-vivo rat study also documented that the stimulation of dopamine D_1 - D_2 receptor heteromers increased brain-derived neurotrophic factor (BDNF) production and neuronal growth in the striatum (Hasbi et al., 2009), raising the possibility that this dopamine-induced BDNF increment backwardly promotes the outgrowth of neurites in cortical neurons constituting the corticostriatal pathway. Because the current study employed a cross-sectional design, a longitudinal morphometric assay during treatment with a D_2 receptor agonist would be necessary for drawing a more decisive conclusion for these regulatory systems. Such investigations should preferably be conducted in healthy subjects, but there would be difficulties in the long-term administration of a D_2 blocker in such individuals.

One of the possible explanations for the present results might be that the number of cortical neurons projecting to the striatum determines the density of D_2 receptors on their presynaptic terminals and the opposite postsynaptic compartments of striatal projection neurons. The nerve fiber and synaptic densities in the corticostriatal tract may regulate the resilience of this network, although the striatal dopaminergic tone, which is functionally linked to the balance between presynaptic and postsynaptic D_2 receptors, could not greatly fluctuate. However, interpretation of our results should be done with caution, as [^{11}C]raclopride BP_{ND} does not solely reflect D_2 receptor density, but is also influenced by other factors such as endogenous dopamine levels and receptor conformation. Our results of partial correlational analyses suggested that the association between brain morphology and D_2 receptors was not explained by DAT availability. The correlation between [^{11}C]raclopride BP_{ND} in the limbic striatal subregion and eigenvariates in the 17 subjects remained at a trend level significance, presumably due to the small sample size, as the r value was similar to the analysis of the whole sample (0.40 in 17 subjects vs. 0.43 in 34 subjects).

In contrast to D_2 receptors, we could not find significant correlations of DAT availability with the GM volumes of any brain regions.

DAT availability is believed to be associated with the density of the nigrostriatal dopaminergic terminals (Hersch, Yi, Heilman, Edwards, & Levey, 1997; Kimmel, Joyce, Carroll, & Kuhar, 2001), but baseline concentrations of synaptically released dopamine, which could act on the corticostriatal nerves as a morphogen, may be stabilized in a manner independent of this density in a healthy, homeostatic condition. In a pathological circumstance causing profound changes in DAT availability, abnormalities of tonic dopamine levels at the synaptic cleft may occur, affecting the morphology of the connected cortical areas. In fact, accumulating evidence suggests that reduced DAT radioligand binding is cross-sectionally and longitudinally associated with cortical atrophy in Parkinson's disease (PD; Sampedro, Marin-Lahoz, Martinez-Horta, Pagonabarraga, & Kulisevsky, 2019; Ye et al., 2018). The underlying condition of cortical atrophy in PD is considered to be as follows. First, impairments of the nigrostriatal pathway give rise to a loss of presynaptic terminals releasing dopamine. Then, the DAT density in the striatum declines, leading to a decrement of the activation of D_2 receptors and spoiling the corticostriatal circuits (Calabresi, Pisani, Centonze, & Bernardi, 1997; Kreitzer & Malenka, 2007; Petzinger et al., 2013; Picconi et al., 2003; Shen, Flajolet, Greengard, & Surmeier, 2008).

The current study is the first to assess the relationships between D_2 receptors and DATs in functional striatal subdivisions. We found positive correlations between the availabilities of these two components in the executive and sensorimotor striatal subregions, presumably reflecting a coupled change in the availabilities of presynaptic and postsynaptic terminals derived from the corticostriatal and nigrostriatal circuit neurons. Such coupling intensity could have diversity among the three subregions, but these data should be considered as being preliminary in light of the relatively small sample size in the present assays. Although the mechanism underlying the reciprocal action between D_2 receptor and DAT is not well clarified, some relevant findings have been reported, as several *in vitro* and *in vivo* studies have revealed that D_2 receptor activation could increase DAT mediated DA clearance and DAT cell-surface expression (Bolan et al., 2007; Cass & Gerhardt, 1994; Mayfield & Zahniser, 2001; Meiergerd, Patterson, & Schenk, 1993); in a rat study, D_2 agonist and antagonist decreased and increased the half-life of DAT in the striatum, respectively, suggesting that dopamine might have influenced DAT turnover through D_2 receptor (Kimmel et al., 2001); another rat study showed that DAT might be regulated by D_2 receptor through a direct protein-protein interaction being independent of D_2 receptor activation (Lee et al., 2007). Conversely, accumulating findings of *in vitro* studies suggest that DAT regulates reuptake, spillover, and diffusion of extracellular dopamine, resulting in activation of D_2 receptor (Chen et al., 2006; Courtney & Ford, 2014).

Our results showed that [^{11}C]raclopride BP_{ND} in each striatal subregion was significantly correlated with GM volumes in regions associated with each function (i.e., limbic, executive, and sensorimotor) and those adjacent areas. The parahippocampal gyrus, being correlated with [^{11}C]raclopride BP_{ND} in the limbic striatal subregion, is considered to be the primary hub of the default mode network in the medial

temporal lobe memory system during resting state (Ward et al., 2014). The temporal cortices adjacent to the limbic system have been reported to have a connection with the ventral-medial anterior caudate in nonhuman primates, although the connection between the temporal lobe and striatum was limited in Tziortzi et al.'s diffusion-weighted MRI study (Selemon & Goldman-Rakic, 1985; Tziortzi et al., 2014). The prefrontal cortex, being correlated with [^{11}C]raclopride BP_{ND} values in the limbic striatal subregion, is known to play a central role in organizing and controlling goal-directed thought and behavior (Szczepanski & Knight, 2014). The supplementary motor cortices and somatosensory cortices, being correlated with [^{11}C]raclopride BP_{ND} values in the sensorimotor striatal subregion, are thought to be crucial in voluntary movement and linking between sensory processing and movement production, respectively (Borich, Brodie, Gray, Ionta, & Boyd, 2015; Nachev, Kennard, & Husain, 2008). Our results suggest that dopamine D_2 receptors in these striatal subregions might be involved in the functioning of these brain regions, respectively. On the other hand, [^{11}C]raclopride BP_{ND} values in each of the striatal subregions were also correlated with regions overlapping with other subregions. This might reflect integrating information between functions with overlapping projections throughout the striatum that enables reward-based and goal-directed behaviors, as indicated previously (Tziortzi et al., 2014). The correlations between BP_{ND} and the eigenvariables were not significantly different among the three subregions when comparing the z-transformed correlation coefficients by two-tailed t-tests (Pearson's r value range, .43–.54; p value range, .57–.96 in the 34 subjects), suggesting that the strength of associations between striatal dopamine D_2 availability and related brain regions might not be markedly different among them. However, to clarify this issue in greater detail, further neuroimaging studies combined with functional/structural connectivity measures will be necessary.

Along with novel findings and implications, there are also some possible limitations in this study. First, we investigated correlations rather than causal relationships between dopamine neurotransmission and brain morphology. Second, we should be careful in interpreting the results because of the small sample size. Third, although the Müller-Gärtner approach corrects the effects of spill-in and spill-out of radioactivity between GM and WM and decreases the influence of striatal brain volume on measured uptake, and our results with PVC are generally consistent with the results without PVC, the Müller-Gärtner approach could not correct the effects of spill-in and spill-out within the three striatal subregions. Fourth, we did not perform a drug screening test on the day of PET acquisition to completely exclude the use of psychoactive substances that can influence D_2 receptor availabilities, although the absence of past and current drug use was confirmed by an interview by a board-certified psychiatrist. Indeed, intake of some psychoactive substances, such as alcohol and caffeine, can influence D_2 receptor availabilities (Nina BL Urban et al., 2010; Volkow et al., 2015). Finally, the limited age range and sex of the participants impeded assessments of the effect of these two parameters. Accordingly, our results should be cautiously interpreted in view of these technical issues.

In conclusion, our results demonstrated differential involvements of DATs and D₂ receptors in the links between cortical morphology and the striatal dopaminergic system via the functional connections. The current findings also suggest unique structural and functional corticostriatal associations in healthy humans, which might be somewhat independent of the nigrostriatal pathway. Similar PET and MRI approaches will provide insights into the implication of the dopamine transmission in the structures of connected regions in neuropsychiatric disorders. It should be of particular significance to conduct these assays in drug-naïve patients with schizophrenia, since aberrant GM volumes and striatal dopaminergic statuses have been reported in this illness (Hajima et al., 2013; Howes et al., 2012).

ACKNOWLEDGMENTS

We thank Kazuko Suzuki and Izumi Kaneko for their assistance as clinical coordinators, Hiromi Sano for her support with MRI scans, and the staff of the Department of Radiopharmaceutics Development for the radioligand synthesis. This work was supported in part by a Grant-in-Aid for Young Scientist (19K17101 to MK) from the Japan Society for the Promotion of Science (JSPS), and by the programs for Brain/MINDS-beyond (19dm0307105 to MH) and Brain Mapping by Integrated Neurotechnologies for Disease Studies (Brain/MINDS; 20dm0207072 to MH) from the Japan Agency for Medical Research and Development. These agencies had no further role in the study design, collection, analysis, or interpretation of the data, the writing of the report, or in the decision to submit the paper for publication.

Dr. Kurose has received research grants from JSPS. Dr. Kubota has received research grants from JSPS, SENSHIN Medical Research Foundation, and Medical Institute of Developmental Disabilities Research, Showa University. Dr. Takahata has received research grants from JSPS and the General Insurance Association of Japan. Dr. Yamamoto has no competing interests to disclose. Dr. Fujiwara has received research grants from JSPS. Dr. Kimura has received research grants from JSPS, Japan Agency for Medical Research and Development (AMED), and National Center for Geriatrics and Gerontology. Dr. Ito has received research grants from JSPS. Dr. Takeuchi has received research grants from JSPS, Japan Agency for Medical Research and Development (AMED), SENSHIN Medical Research Foundation, and Novartis Pharma; fellowship grants from Astellas Foundation for Research on Metabolic Disorders, the Canadian Institutes of Health Research (CIHR), Centre for Addiction and Mental Health (CAMH) Foundation, and the Japanese Society of Clinical Neuropsychopharmacology (JSCNP); speaker's fees from Kyowa, Janssen, Meiji Seika Pharma, Mochida, Otsuka, Sumitomo Dainippon Pharma, and Yoshitomiyakuhin; and manuscript fees from Sumitomo Dainippon Pharma. Dr. Mimura has received research grants from JSPS, AMED and Japan Ministry of Health, Labour and Welfare. Dr. Suhara has received research grants from AMED and Japan Ministry of Health, Labour and Welfare. Dr. Higuchi has received research grants from JSPS, AMED and Japan Ministry of Health, Labour and Welfare.

CONFLICT OF INTERESTS

The authors have no conflicts of interest directly relevant to the content of this article.

AUTHOR CONTRIBUTIONS

Manabu Kubota conceived the original idea. Hironobu Fujiwara, Yasuyuki Kimura, and Hiroshi Ito carried out the experiments. Shin Kurose and Manabu Kubota analyzed the data and wrote the first draft. Shin Kurose, Manabu Kubota, Keisuke Takahata, Yasuharu Yamamoto, Hiroyoshi Takeuchi, and Makoto Higuchi contributed to the interpretation of the results. Makoto Higuchi supervised the project. All authors have made substantial intellectual contribution to the work and approved the final manuscript.

DATA AVAILABILITY STATEMENT

The data that support the findings of this study are available from the corresponding author upon reasonable request.

ORCID

Shin Kurose  <https://orcid.org/0000-0001-8355-4946>

Manabu Kubota  <https://orcid.org/0000-0001-9507-1845>

Yasuharu Yamamoto  <https://orcid.org/0000-0002-1954-8004>

REFERENCES

- Abi-Dargham, A., Rodenhiser, J., Printz, D., Zea-Ponce, Y., Gil, R., Kegeles, L. S., ... Laruelle, M. (2000). Increased baseline occupancy of D₂ receptors by dopamine in schizophrenia. *Proceedings of the National Academy of Sciences of the United States of America*, 97(14), 8104–8109. <https://doi.org/10.1073/pnas.97.14.8104>
- Alakurtti, K., Johansson, J. J., Joutsa, J., Laine, M., Bäckman, L., Nyberg, L., & Rinne, J. O. (2015). Long-term test–retest reliability of striatal and extrastriatal dopamine D_{2/3} receptor binding: Study with [¹¹C] raclopride and high-resolution PET. *Journal of Cerebral Blood Flow & Metabolism*, 35(7), 1199–1205.
- Alexander, G. E., DeLong, M. R., & Strick, P. L. (1986). Parallel organization of functionally segregated circuits linking basal ganglia and cortex. *Annual Review of Neuroscience*, 9(1), 357–381.
- Ashburner, J. (2007). A fast diffeomorphic image registration algorithm. *NeuroImage*, 38(1), 95–113.
- Ashburner, J., & Friston, K. J. (2000). Voxel-based morphometry—The methods. *NeuroImage*, 11(6 Pt 1), 805–821. <https://doi.org/10.1006/nimg.2000.0582>
- Boileau, I., Payer, D., Chugani, B., Lobo, D., Behzadi, A., Rusjan, P. M., ... Kish, S. J. (2013). The D_{2/3} dopamine receptor in pathological gambling: A positron emission tomography study with [¹¹C]-(-)-propylhexahydro-naphtho-oxazin and [¹¹C] raclopride. *Addiction*, 108(5), 953–963.
- Bolan, E. A., Kivell, B., Jaligam, V., Oz, M., Jayanthi, L. D., Han, Y., ... Shippenberg, T. S. (2007). D₂ receptors regulate dopamine transporter function via an extracellular signal-regulated kinases 1 and 2-dependent and phosphoinositide 3 kinase-independent mechanism. *Molecular Pharmacology*, 71(5), 1222–1232. <https://doi.org/10.1124/mol.106.027763>
- Borich, M., Brodie, S., Gray, W., Ionta, S., & Boyd, L. (2015). Understanding the role of the primary somatosensory cortex: Opportunities for rehabilitation. *Neuropsychologia*, 79, 246–255.
- Calabresi, P., Pisani, A., Centonze, D., & Bernardi, G. (1997). Synaptic plasticity and physiological interactions between dopamine and glutamate

- in the striatum. *Neuroscience and Biobehavioral Reviews*, 21(4), 519–523.
- Caravaggio, F., Borlido, C., Wilson, A., & Graff-Guerrero, A. (2015). Examining endogenous dopamine in treated schizophrenia using [(11)C]-(+)-PHNO positron emission tomography: A pilot study. *Clinica Chimica Acta*, 449, 60–62. <https://doi.org/10.1016/j.cca.2015.03.020>
- Caravaggio, F., Ku Chung, J., Plitman, E., Boileau, I., Gerretsen, P., Kim, J., ... Graff-Guerrero, A. (2017). The relationship between subcortical brain volume and striatal dopamine D2/3 receptor availability in healthy humans assessed with [(11) C]-raclopride and [(11) C]-(+)-PHNO PET. *Human Brain Mapping*, 38(11), 5519–5534. <https://doi.org/10.1002/hbm.23744>
- Cass, W. A., & Gerhardt, G. A. (1994). Direct in vivo evidence that D2 dopamine receptors can modulate dopamine uptake. *Neuroscience Letters*, 176(2), 259–263. [https://doi.org/10.1016/0304-3940\(94\)90096-5](https://doi.org/10.1016/0304-3940(94)90096-5)
- Chen, R., Tilley, M. R., Wei, H., Zhou, F., Zhou, F.-M., Ching, S., ... Gu, H. H. (2006). Abolished cocaine reward in mice with a cocaine-insensitive dopamine transporter. *Proceedings of the National Academy of Sciences*, 103(24), 9333–9338. <https://doi.org/10.1073/pnas.0600905103>
- Courtney, N. A., & Ford, C. P. (2014). The timing of dopamine- and noradrenaline-mediated transmission reflects underlying differences in the extent of spillover and pooling. *The Journal of Neuroscience*, 34(22), 7645–7656. <https://doi.org/10.1523/jneurosci.0166-14.2014>
- Diedrichsen, J., Balsters, J. H., Flavell, J., Cussans, E., & Ramnani, N. (2009). A probabilistic MR atlas of the human cerebellum. *NeuroImage*, 46(1), 39–46.
- Draganski, B., Kherif, F., Kloppel, S., Cook, P. A., Alexander, D. C., Parker, G. J., ... Frackowiak, R. S. (2008). Evidence for segregated and integrative connectivity patterns in the human basal ganglia. *The Journal of Neuroscience*, 28(28), 7143–7152. <https://doi.org/10.1523/jneurosci.1486-08.2008>
- Gallezot, J. D., Beaver, J. D., Gunn, R. N., Nabulsi, N., Weinzimmer, D., Singhal, T., ... Huang, Y. (2012). Affinity and selectivity of [(11)C]-(+)-PHNO for the D3 and D2 receptors in the rhesus monkey brain in vivo. *Synapse*, 66(6), 489–500.
- Haber, S. N. (2003). The primate basal ganglia: Parallel and integrative networks. *Journal of Chemical Neuroanatomy*, 26(4), 317–330.
- Hajima, S. V., Van Haren, N., Cahn, W., Koolschijn, P. C., Hulshoff Pol, H. E., & Kahn, R. S. (2013). Brain volumes in schizophrenia: A meta-analysis in over 18 000 subjects. *Schizophrenia Bulletin*, 39(5), 1129–1138. <https://doi.org/10.1093/schbul/sbs118>
- Hasbi, A., Fan, T., Aljaniaram, M., Nguyen, T., Perreault, M. L., O'Dowd, B. F., & George, S. R. (2009). Calcium signaling cascade links dopamine D1–D2 receptor heteromer to striatal BDNF production and neuronal growth. *Proceedings of the National Academy of Sciences*, 106(50), 21377–21382. <https://doi.org/10.1073/pnas.0903676106>
- Hersch, S. M., Yi, H., Heilman, C. J., Edwards, R. H., & Levey, A. I. (1997). Subcellular localization and molecular topology of the dopamine transporter in the striatum and substantia nigra. *The Journal of Comparative Neurology*, 388(2), 211–227.
- Honea, R., Crow, T. J., Passingham, D., & Mackay, C. E. (2005). Regional deficits in brain volume in schizophrenia: A meta-analysis of voxel-based morphometry studies. *The American Journal of Psychiatry*, 162(12), 2233–2245. <https://doi.org/10.1176/appi.ajp.162.12.2233>
- Howes, O. D., Kambeitz, J., Kim, E., Stahl, D., Slifstein, M., Abi-Dargham, A., & Kapur, S. (2012). The nature of dopamine dysfunction in schizophrenia and what this means for treatment. *Archives of General Psychiatry*, 69(8), 776–786. <https://doi.org/10.1001/archgenpsychiatry.2012.169>
- Ishikawa, A., Kitamura, K., Mizuta, T., Tanaka, K., Amano, M., Inoue, Y., ... Senda, M. (2005). Implementation of on-the-fly scatter correction using dual energy window method in continuous 3D whole body PET scanning. Paper presented at the IEEE Nuclear Science Symposium Conference Record, 2005.
- Ito, H., Shinotoh, H., Shimada, H., Miyoshi, M., Yanai, K., Okamura, N., ... Kodaka, F. (2014). Imaging of amyloid deposition in human brain using positron emission tomography and [18 F] FACT: Comparison with [11 C] PIB. *European Journal of Nuclear Medicine and Molecular Imaging*, 41(4), 745–754.
- Jaworska, N., Cox, S. M., Casey, K. F., Boileau, I., Cherkasova, M., Larcher, K., ... Leyton, M. (2017). Is there a relation between novelty seeking, striatal dopamine release and frontal cortical thickness? *PLoS One*, 12(3), e0174219. <https://doi.org/10.1371/journal.pone.0174219>
- Kegeles, L. S., Abi-Dargham, A., Frankle, W. G., Gil, R., Cooper, T. B., Slifstein, M., ... Laruelle, M. (2010). Increased synaptic dopamine function in associative regions of the striatum in schizophrenia. *Archives of General Psychiatry*, 67(3), 231–239. <https://doi.org/10.1001/archgenpsychiatry.2010.10>
- Kimmel, H. L., Joyce, A. R., Carroll, F. I., & Kuhar, M. J. (2001). Dopamine D1 and D2 receptors influence dopamine transporter synthesis and degradation in the rat. *The Journal of Pharmacology and Experimental Therapeutics*, 298(1), 129–140. Retrieved from <https://pubmed.ncbi.nlm.nih.gov/11408534>
- Kimura, Y., Maeda, J., Yamada, M., Takahata, K., Yokokawa, K., Ikoma, Y., ... Sahara, T. (2017). Measurement of psychological state changes at low dopamine transporter occupancy following a clinical dose of mazindol. *Psychopharmacology*, 234(3), 323–328. <https://doi.org/10.1007/s00213-016-4464-x>
- Kreitzer, A. C., & Malenka, R. C. (2007). Endocannabinoid-mediated rescue of striatal LTD and motor deficits in Parkinson's disease models. *Nature*, 445(7128), 643–647. <https://doi.org/10.1038/nature05506>
- Lammertsma, A. A., & Hume, S. P. (1996). Simplified reference tissue model for PET receptor studies. *NeuroImage*, 4(3 Pt 1), 153–158. <https://doi.org/10.1006/nimg.1996.0066>
- Lee, F. J., Pei, L., Moszczynska, A., Vukusic, B., Fletcher, P. J., & Liu, F. (2007). Dopamine transporter cell surface localization facilitated by a direct interaction with the dopamine D2 receptor. *The EMBO Journal*, 26(8), 2127–2136. <https://doi.org/10.1038/sj.emboj.7601656>
- Mayfield, R. D., & Zahniser, N. R. (2001). Dopamine D2 receptor regulation of the dopamine transporter expressed in *Xenopus laevis* oocytes is voltage-independent. *Molecular Pharmacology*, 59(1), 113–121. <https://doi.org/10.1124/mol.59.1.113>
- Mecca, A. P., Barcelos, N. M., Wang, S., Brück, A., Nabulsi, N., Planeta-Wilson, B., ... Huang, Y. (2018). Cortical β -amyloid burden, gray matter, and memory in adults at varying APOE ϵ 4 risk for Alzheimer's disease. *Neurobiology of Aging*, 61, 207–214.
- Mecca, A. P., McDonald, J. W., Michalak, H. R., Godek, T. A., Harris, J. E., Pugh, E. A., ... Nabulsi, N. B. (2020). PET imaging of mGluR5 in Alzheimer's disease. *Alzheimer's Research & Therapy*, 12(1), 1–10.
- Meiergerd, S. M., Patterson, T. A., & Schenk, J. O. (1993). D2 receptors may modulate the function of the striatal transporter for dopamine: Kinetic evidence from studies in vitro and in vivo. *Journal of Neurochemistry*, 61(2), 764–767. <https://doi.org/10.1111/j.1471-4159.1993.tb02185.x>
- Mukherjee, J., Christian, B. T., Dunigan, K. A., Shi, B., Narayanan, T. K., Satter, M., & Mantil, J. (2002). Brain imaging of 18F-fallypride in normal volunteers: Blood analysis, distribution, test-retest studies, and preliminary assessment of sensitivity to aging effects on dopamine D-2/D-3 receptors. *Synapse*, 46(3), 170–188.
- Müller-Gärtner, H. W., Links, J. M., Prince, J. L., Bryan, R. N., McVeigh, E., Leal, J. P., ... Frost, J. J. (1992). Measurement of radiotracer concentration in brain gray matter using positron emission tomography: MRI-based correction for partial volume effects. *Journal of Cerebral Blood Flow & Metabolism*, 12(4), 571–583.

- Nachev, P., Kennard, C., & Husain, M. (2008). Functional role of the supplementary and pre-supplementary motor areas. *Nature Reviews. Neuroscience*, 9(11), 856–869. <https://doi.org/10.1038/nrn2478>
- Parent, A., & Hazrati, L. N. (1995). Functional anatomy of the basal ganglia. I. the cortico-basal ganglia-thalamo-cortical loop. *Brain Research Reviews*, 20(1), 91–127.
- Petzinger, G. M., Fisher, B. E., McEwen, S., Beeler, J. A., Walsh, J. P., & Jakowec, M. W. (2013). Exercise-enhanced neuroplasticity targeting motor and cognitive circuitry in Parkinson's disease. *Lancet Neurology*, 12(7), 716–726. [https://doi.org/10.1016/s1474-4422\(13\)70123-6](https://doi.org/10.1016/s1474-4422(13)70123-6)
- Picconi, B., Centonze, D., Håkansson, K., Bernardi, G., Greengard, P., Fisone, G., ... Calabresi, P. (2003). Loss of bidirectional striatal synaptic plasticity in L-DOPA-induced dyskinesia. *Nature Neuroscience*, 6(5), 501–506. <https://doi.org/10.1038/nn1040>
- Reynolds, J. N., & Wickens, J. R. (2002). Dopamine-dependent plasticity of corticostriatal synapses. *Neural Networks*, 15(4–6), 507–521. [https://doi.org/10.1016/s0893-6080\(02\)00045-x](https://doi.org/10.1016/s0893-6080(02)00045-x)
- Sampedro, F., Marin-Lahoz, J., Martinez-Horta, S., Pagonabarraga, J., & Kulisevsky, J. (2019). Dopaminergic degeneration induces early posterior cortical thinning in Parkinson's disease. *Neurobiology of Disease*, 124, 29–35. <https://doi.org/10.1016/j.nbd.2018.11.001>
- Selemon, L. D., & Goldman-Rakic, P. S. (1985). Longitudinal topography and interdigitation of corticostriatal projections in the rhesus monkey. *The Journal of Neuroscience*, 5(3), 776–794.
- Shen, W., Flajolet, M., Greengard, P., & Surmeier, D. J. (2008). Dichotomous dopaminergic control of striatal synaptic plasticity. *Science*, 321(5890), 848–851. <https://doi.org/10.1126/science.1160575>
- Shepherd, A. M., Laurens, K. R., Matheson, S. L., Carr, V. J., & Green, M. J. (2012). Systematic meta-review and quality assessment of the structural brain alterations in schizophrenia. *Neuroscience and Biobehavioral Reviews*, 36(4), 1342–1356. <https://doi.org/10.1016/j.neubiorev.2011.12.015>
- Strafella, A. P., Paus, T., Barrett, J., & Dagher, A. (2001). Repetitive transcranial magnetic stimulation of the human prefrontal cortex induces dopamine release in the caudate nucleus. *Journal of Neuroscience*, 21(15), RC157. <https://doi.org/10.1523/JNEUROSCI.21-15-j0003.2001>, 21, RC157
- Strafella, A. P., Paus, T., Fraraccio, M., & Dagher, A. (2003). Striatal dopamine release induced by repetitive transcranial magnetic stimulation of the human motor cortex. *Brain*, 126(Pt 12), 2609–2615. <https://doi.org/10.1093/brain/awg268>
- Szczepanski, S. M., & Knight, R. T. (2014). Insights into human behavior from lesions to the prefrontal cortex. *Neuron*, 83(5), 1002–1018.
- Todd, R. D. (1992). Neural development is regulated by classical neurotransmitters: Dopamine D2 receptor stimulation enhances neurite outgrowth. *Biological Psychiatry*, 31(8), 794–807.
- Tziortzi, A. C., Haber, S. N., Searle, G. E., Tsoumpas, C., Long, C. J., Shotbolt, P., ... Gunn, R. N. (2014). Connectivity-based functional analysis of dopamine release in the striatum using diffusion-weighted MRI and positron emission tomography. *Cerebral Cortex*, 24(5), 1165–1177. <https://doi.org/10.1093/cercor/bhs397>
- Urban, N. B., Kegeles, L. S., Slifstein, M., Xu, X., Martinez, D., Sakr, E., ... Krystal, J. H. (2010). Sex differences in striatal dopamine release in young adults after oral alcohol challenge: A positron emission tomography imaging study with [11C] raclopride. *Biological Psychiatry*, 68(8), 689–696.
- Urban, N. B., Slifstein, M., Thompson, J. L., Xu, X., Girgis, R. R., Raheja, S., ... Abi-Dargham, A. (2012). Dopamine release in chronic cannabis users: A [11c]raclopride positron emission tomography study. *Biological Psychiatry*, 71(8), 677–683. <https://doi.org/10.1016/j.biopsych.2011.12.018>
- Volkow, N., Wang, G., Logan, J., Alexoff, D., Fowler, J., Thanos, P., ... Tomasi, D. (2015). Caffeine increases striatal dopamine D2/D3 receptor availability in the human brain. *Translational Psychiatry*, 5(4), e549–e549.
- Wall, N. R., De La Parra, M., Callaway, E. M., & Kreitzer, A. C. (2013). Differential innervation of direct and indirect-pathway striatal projection neurons. *Neuron*, 79(2), 347–360.
- Ward, A. M., Schultz, A. P., Huijbers, W., Van Dijk, K. R., Hedden, T., & Sperling, R. A. (2014). The parahippocampal gyrus links the default-mode cortical network with the medial temporal lobe memory system. *Human Brain Mapping*, 35(3), 1061–1073.
- Woodward, N. D., Zald, D. H., Ding, Z., Riccardi, P., Ansari, M. S., Baldwin, R. M., ... Kessler, R. M. (2009). Cerebral morphology and dopamine D2/D3 receptor distribution in humans: A combined [18F] fallypride and voxel-based morphometry study. *NeuroImage*, 46(1), 31–38. <https://doi.org/10.1016/j.neuroimage.2009.01.049>
- Yao, L., Lui, S., Liao, Y., Du, M. Y., Hu, N., Thomas, J. A., & Gong, Q. Y. (2013). White matter deficits in first episode schizophrenia: An activation likelihood estimation meta-analysis. *Progress in Neuro-Psychopharmacology & Biological Psychiatry*, 45, 100–106. <https://doi.org/10.1016/j.pnpbp.2013.04.019>
- Ye, B. S., Jeon, S., Yoon, S., Kang, S. W., Baik, K., Lee, Y., ... Sohn, Y. H. (2018). Effects of dopaminergic depletion and brain atrophy on neuropsychiatric symptoms in de novo Parkinson's disease. *Journal of Neurology, Neurosurgery, and Psychiatry*, 89(2), 197–204. <https://doi.org/10.1136/jnnp-2017-316075>
- Zhang, X., Bearer, E. L., Boulat, B., Hall, F. S., Uhl, G. R., & Jacobs, R. E. (2010). Altered neurocircuitry in the dopamine transporter knockout mouse brain. *PLoS One*, 5(7), e11506.

SUPPORTING INFORMATION

Additional supporting information may be found online in the Supporting Information section at the end of this article.

How to cite this article: Kurose, S., Kubota, M., Takahata, K., Yamamoto, Y., Fujiwara, H., Kimura, Y., Ito, H., Takeuchi, H., Mimura, M., Suhara, T., & Higuchi, M. (2021). Relationship between regional gray matter volumes and dopamine D₂ receptor and transporter in living human brains. *Human Brain Mapping*, 42(12), 4048–4058. <https://doi.org/10.1002/hbm.25538>